Bipolar Poisson Solution for Independent Double-Gate MOSFET

Aby Abraham, Pankaj Kumar Thakur, and Santanu Mahapatra, *Senior Member, IEEE*

***Abstract*—We propose a new set of input voltage equations (IVEs) for independent double-gate MOSFET by solving the governing bipolar Poisson equation (PE) rigorously. The proposed IVEs, which involve the Legendre's incomplete elliptic integral of the first kind and Jacobian elliptic functions and are valid from accumulation to inversion regimes, are shown to have good agreement with the numerical solution of the same PE for all bias conditions.**

***Index Terms*—Compact modeling, independent double-gate (IDG) MOSFET, Poisson solution.**

I. Introduction

EXISTING surface-potential-based compact models for the undoped-body independent double-gate (IDG) MOSFET [1]–[4] are based on the input voltage equations (IVEs) derived from the unipolar (considering either electron or hole concentration) approximation of the governing 1-D Poisson equation (PE) [5]. Although it yields sufficiently accurate results for most practical cases (i.e., inversion mode operation), one needs IVEs that are valid from accumulation-to-inversion regime for the completeness of the model, to improve the accuracy near the flatband condition, and for varactor applications [6]. IVEs based on the solution of bipolar PE have recently been reported for symmetric DG MOSFETs in [7] and [8]; however, no such solution has been reported for the IDG MOSFET.

In this brief, we propose a new set of IVEs by solving the bipolar PE rigorously, which is valid from accumulation to inversion regime. In an analogy to the earlier proposed IVEs based on the unipolar approximation [5], it is shown that the device behavior is again dictated by different sets of IVEs based on the bias conditions. The electrostatic potential calculated from these IVEs is shown to have good agreement with the numerical solution under all bias conditions.

II. Solution Technique and Results

The conventions used in this brief are as follows: $C_{\mathrm{ox1(2)}}$ is the oxide capacitance per unit area of the first (second) gate defined as $\epsilon_{\mathrm{ox}}/t_{\mathrm{ox1(2)}}$; C_{si} is the silicon body capacitance per unit area defined as $\varepsilon_{\mathrm{si}}/t_{\mathrm{si}}$; $\varepsilon_{\mathrm{si}}$ and $\varepsilon_{\mathrm{ox}}$ are the permittivities; t_{si} and t_{ox} are the thicknesses of silicon and SiO_2 films, respectively; q is the elementary charge; β is the inverse thermal voltage; n_i is the intrinsic carrier density; V is the electron quasi-Fermi potential (channel potential); $\psi_{1(2)}$ is the Si/SiO_2 interface potential at the first (second) gate; and $V_{g1(2)}$ is the effective front (back)-gate voltage, i.e., $V_{g1(2)} = V_{g1(2)\mathrm{applied}} - \Delta\phi_{1(2)}$, where $\Delta\phi_{1(2)}$ is the work function difference at the respective gates. In the following discussion, superscripts "BP" and "UP" refer to "bipolar" and "unipolar" cases, respectively.

Under the gradual channel approximation, the governing bipolar PE for DG MOSFET could be written as in [7], [8]

$$\frac{d^2\psi}{dy^2} = \frac{2qn_i}{\varepsilon_{\mathrm{si}}} e^{-\beta\frac{V}{2}} \sinh\left(\beta\left(\psi - \frac{V}{2}\right)\right) \tag{1}$$

with the boundary conditions BC1 and BC2 as given in [5]. Using the same approach [5], on integrating (1) with BC1 and BC2 as the lower limit, we obtain

$$\frac{d\psi}{dy} = \pm\sqrt{2Ae^{\beta\frac{V}{2}}\left[\cosh\left(\beta\left(\psi - \frac{V}{2}\right)\right) + G_1^{\mathrm{BP}}\right]} \tag{2}$$

$$\frac{d\psi}{dy} = \pm\sqrt{2Ae^{\beta\frac{V}{2}}\left[\cosh\left(\beta\left(\psi - \frac{V}{2}\right)\right) + G_2^{\mathrm{BP}}\right]} \tag{3}$$

where $A{=}2qn_ie^{-\beta V}/\varepsilon_{\mathrm{si}}\beta$ and $G_{1(2)}^{\mathrm{BP}}{=}[(C_{\mathrm{ox1(2)}}/\varepsilon_{\mathrm{si}})^2(V_{g1(2)} - \psi_{1(2)})^2/2Ae^{\beta(V/2)}] - \cosh(\beta(\psi_{1(2)} - (V/2)))$. Here, $G_{1(2)}^{\mathrm{BP}}$ is analogous to $G_{1(2)}^{\mathrm{UP}}$ defined in [5], and it can be seen that $2Ae^{\beta(V/2)}G_{1(2)}^{\mathrm{BP}} = G_{1(2)}^{\mathrm{UP}}$ when we make the unipolar approximation and replace $\cosh(\beta(\psi_{1(2)} - (V/2)))$ with $(1/2)e^{(\beta(\psi_{1(2)} - (V/2)))}$. Now, we integrate (2) once again with BC1 as the lower limit after discarding the positive sign on the RHS to arrive at three different forms of potential solutions (4)–(6) based on the values of G_1^{BP}

$$G_1^{\mathrm{BP}} > 1 : \psi(y) = \frac{2}{\beta}\tanh^{-1}\left(\mathrm{sn}(u_1, k_1)\right) + \frac{V}{2} \tag{4}$$

where $u_1 = [F(t_1, k_1) - \beta(y + (t_{\mathrm{si}}/2))\sqrt{Ae^{\beta(V/2)}/(1 - k_1^2)}]$, $k_1 = \sqrt{(G_1^{\mathrm{BP}} - 1)/(G_1^{\mathrm{BP}} + 1)}$, and $t_1 = \sin^{-1}[\tanh(\beta(\psi_1 - (V/2)))]$

$$\left|G_1^{\mathrm{BP}}\right| \leq 1 : \psi(y) = \frac{2\eta_1}{\beta}\mathrm{sech}^{-1}\left(\mathrm{sn}(u_1, k_1)\right) + \frac{V}{2} \tag{5}$$

Manuscript received August 7, 2012; accepted October 4, 2012. Date of publication November 12, 2012; date of current version December 19, 2012. This work was supported by the Department of Science and Technology, Government of India, under the Ramanna Fellowship program under Grant SR/S3/EECE/0123/2011. The review of this brief was arranged by Editor M. J. Kumar.

A. Abraham is with Intel Technology India Pvt. Ltd., Bangalore 560017, India (e-mail: aby.abraham@intel.com).

P. K. Thakur and S. Mahapatra are with the Nano Scale Device Research Laboratory, Department of Electronic Systems Engineering (formerly CEDT), Indian Institute of Science, Bangalore 560012, India (e-mail: pankaj@cedt.iisc.ernet.in; santanu@cedt.iisc.ernet.in).

Color versions of one or more of the figures in this brief are available online at http://ieeexplore.ieee.org.

Digital Object Identifier 10.1109/TED.2012.2223703

where $u_1 = [F(t_1, k_1) + \eta_1 \beta(y + (t_{si}/2))\sqrt{Ae^{\beta(V/2)}}]$, $k_1 = \sqrt{(1 - G_1^{BP})/2}$, and $t_1 = \sin^{-1}[\text{sech}(\beta(\psi_1 - (V/2)))]$

$$G_1^{BP} < -1 : \psi(y) = \frac{2\eta_1}{\beta} \log\left(\frac{e^{\frac{\theta}{2}}}{\text{sn}(u_1, k_1)}\right) + \frac{V}{2} \quad (6)$$

where $u_1 = [F(t_1, k_1) + \eta_1(\beta/2)(y + (t_{si}/2))\sqrt{Ae^{\beta(V/2)}/k_1}]$, $k_1 = e^{-\theta}$, $t_1 = \sin^{-1}[e^{((\theta/2) - \eta_1(\beta/2)(\psi_1 - (V/2)))}]$, $\theta = \cosh^{-1}(G_1^{*BP})$, and $G_1^{*BP} = -G_1^{BP}$.

In (5) and (6), $\eta_1 = \text{sgn}(\beta(\psi_1 - (V/2)))$ and $F(t, k)$ is the Legendre's incomplete elliptic integral of the first kind given by

$$u = F(t, k) = \int_0^t \frac{d\theta}{\sqrt{1 - k^2 \sin^2(\theta)}}. \quad (7)$$

$\text{sn}(u, k)$, $\text{cn}(u, k)$, and $\text{dn}(u, k)$ are the Jacobian elliptic functions defined as $\text{sn}(u, k) = \sin(t)$, $\text{cn}(u, k) = \cos(t)$, and $\text{dn}(u, k) = \sqrt{1 - k^2 \text{sn}^2(u, k)}$ for $t = \text{am}(u, k)$, with "$\text{am}(u, k)$" denoting the Jacobi amplitude (inverse of the incomplete elliptic integral of the first kind)[9].

Similarly, integrating (3) with BC2 as the lower limit after discarding the negative sign on RHS, we arrive at another set of potential solutions (8)–(10) based on the values of G_2^{BP}

$$G_2^{BP} > 1 : \psi(y) = \frac{2}{\beta} \tanh^{-1}(\text{sn}(u_2, k_2)) + \frac{V}{2} \quad (8)$$

$$\left|G_2^{BP}\right| \le 1 : \psi(y) = \frac{2\eta_2}{\beta} \text{sech}^{-1}(\text{sn}(u_2, k_2)) + \frac{V}{2} \quad (9)$$

$$G_2^{BP} < -1 : \psi(y) = \frac{2\eta_2}{\beta} \log\left(\frac{e^{\frac{\theta}{2}}}{\text{sn}(u_2, k_2)}\right) + \frac{V}{2}. \quad (10)$$

Here, $\eta_2 = \text{sgn}(\beta(\psi_2 - (V/2)))$ and u_2 is obtained by replacing (y, k_1, η_1) with $(-y, k_2, \eta_2)$ in the expression of u_1. Similarly, ψ_1 and η_1 are replaced by ψ_2 and η_2, respectively, in the expression of t_1. To obtain k_2, G_1^{BP} is replaced by G_2^{BP} in the expression of k_1, and G_1^{*BP} is replaced by G_2^{*BP} in the expression of θ.

To derive the IVE, we apply the remaining boundary condition, i.e., BC2 to (4)–(6) and BC1 to (8)–(10), respectively. This results in the set of implicit equations (11)–(13) with u_1 and u_2 being evaluated at $y = t_{si}/2$ and $y = -t_{si}/2$, respectively. Using the forms $\text{cd}(u, k) = (\text{cn}(u, k)/\text{dn}(u, k))$ and $\text{sd}(u, k) = (\text{sn}(u, k)/\text{dn}(u, k))$, this new set of IVEs could be written as

$$G_{1(2)}^{BP} > 1 : V_{g2(1)} - \frac{2}{\beta} \tanh^{-1}\left(\text{sn}\left(u_{1(2)}, k_{1(2)}\right)\right) - \frac{V}{2} = \frac{-2\varepsilon_{si}}{C_{ox2(1)} \text{cd}\left(u_{1(2)}, k_{1(2)}\right)} \sqrt{\frac{Ae^{\beta\frac{V}{2}}}{1 - k_{1(2)}^2}} \quad (11)$$

$$|G_{1(2)}^{BP}| \le 1 : V_{g2(1)} - \frac{2\eta_{1(2)}}{\beta} \text{sech}^{-1}\left(\text{sn}\left(u_{1(2)}, k_{1(2)}\right)\right) - \frac{V}{2} = \frac{-2\varepsilon_{si}}{C_{ox2(1)} \text{sd}\left(u_{1(2)}, k_{1(2)}\right)} \sqrt{Ae^{\beta\frac{V}{2}}} \quad (12)$$

$$G_{1(2)}^{BP} < -1 : V_{g2(1)} - \frac{2\eta_{1(2)}}{\beta} \log\left(\frac{e^{\frac{\theta}{2}}}{\text{sn}\left(u_{1(2)}, k_{1(2)}\right)}\right) - \frac{V}{2} = \frac{-\varepsilon_{si} \text{cn}\left(u_{1(2)}, k_{1(2)}\right)}{C_{ox2(1)} \text{sd}\left(u_{1(2)}, k_{1(2)}\right)} \sqrt{\frac{Ae^{\beta\frac{V}{2}}}{k_{1(2)}}}. \quad (13)$$

It must be noted that we solve one of the IVEs (11)–(13) for the variable $\psi_{1(2)}$ whenever $|V_{g1(2)}| > |V_{g2(1)}|$ and $V_{g1(2)} \ge 0$. If $|V_{g1}| = |V_{g2}|$ and $V_{g1} \ge 0$, we may solve for either ψ_1 or ψ_2. For the remaining cases, i.e., $|V_{g1(2)}| > |V_{g2(1)}|$ with $V_{g1(2)} < 0$, we need to integrate (2) after discarding the negative sign and (3) after discarding the positive sign, respectively, to obtain the necessary IVEs.

Now, as in [5], we introduce the concept of G^{BP}-zero-point (G^{BP}ZP) and critical gate voltage to explain the choice of IVE to be solved for any given bias condition. The implicit equation (obtained by substituting $G_{1(2)}^{BP} = 0$) to be solved to determine the value of $\psi_{gzp1(2)}^{BP}$ could be given as

$$\frac{\left[\frac{C_{ox1(2)}}{\varepsilon_{si}}\left(V_{g1(2)} - \psi_{gzp1(2)}^{BP}\right)\right]^2}{2Ae^{(\beta\frac{V}{2})}} - \cosh\left(\beta\left(\psi_{gzp1(2)}^{BP} - \frac{V}{2}\right)\right) = 0. \quad (14)$$

It can be shown that the aforementioned equation reduces to the explicit formulation for $\psi_{gzp1(2)}^{UP}$ in [5] by replacing $\cosh(\beta(\psi_{gzp1(2)}^{BP} - (V/2)))$ with $(1/2)e^{(\beta(\psi_{gzp1(2)}^{UP} - (V/2)))}$ and $\psi_{gzp1(2)}^{BP}$ with $\psi_{gzp1(2)}^{UP}$.

The expression for $V_{g2(1)crit}^{BP}$ can be obtained by substituting $G_{1(2)}^{BP}$ as zero and $\psi_{1(2)}$ as $\psi_{gzp1(2)}^{BP}$ in (12) as shown in the following:

$$V_{g2(1)crit}^{BP} = \frac{2\eta_{1(2)}}{\beta} \text{sech}^{-1}\left(\text{sn}\left(u_{1(2)}, \frac{1}{\sqrt{2}}\right)\right) + \frac{V}{2} - \frac{\varepsilon_{si}}{C_{ox2(1)}}\left[\frac{2\sqrt{Ae^{\beta\frac{V}{2}}}}{\text{sd}(u_{1(2)}, \frac{1}{\sqrt{2}})}\right]. \quad (15)$$

Now, for $V_{g2(1)} < V_{g2(1)crit}^{BP}$, we solve (11) or (12) as $G_{1(2)}^{BP} > 0$. Similarly, for $V_{g2(1)} \ge V_{g2(1)crit}^{BP}$, (12) or (13) needs to be solved as $G_{1(2)}^{BP} \le 0$. It is important to note that (12) needs to be solved only in a few number of cases when it is found that $|G_{1(2)}^{BP}| \le 1$ during evaluation. However, as typically $|G_{1(2)}^{BP}| \gg 1$, one among (11) or (13) is required to be solved most often. In analogy with the *hyperbolic* ($G_{1(2)}^{UP} > 0$) and *trigonometric* ($G_{1(2)}^{UP} \le 0$) forms of IVEs given in [5], (11) and (13) can be seen to belong exclusively to the *hyperbolic-BP* ($G_{1(2)}^{BP} > 0$) and *trigonometric-BP* ($G_{1(2)}^{BP} \le 0$) regions, respectively. The additional IVE (12) defined for $|G_{1(2)}^{BP}| \le 1$ is part of both the *hyperbolic-BP* and *trigonometric-BP* regions and analogous to (17) and (18) in [5].

The bounds of the solution space [10] for the new bipolar IVEs are formulated here for $V_{g1} \ge V_{g2}$ and are extendible for $V_{g2} > V_{g1}$ along similar lines. For the *hyperbolic-BP* region ($G_1^{BP} > 0$), the upper bound is ψ_{gzp1}^{BP}, while the lower bound is

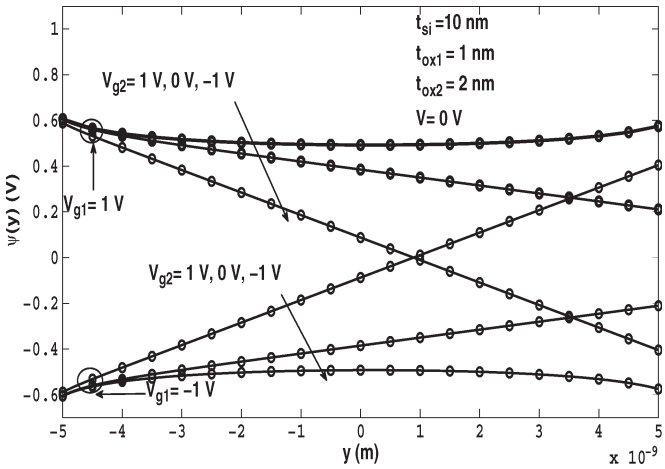

Fig. 1. Potential profile inside the silicon film predicted by the (line) analytical and (symbol) numerical solution for various bias conditions.

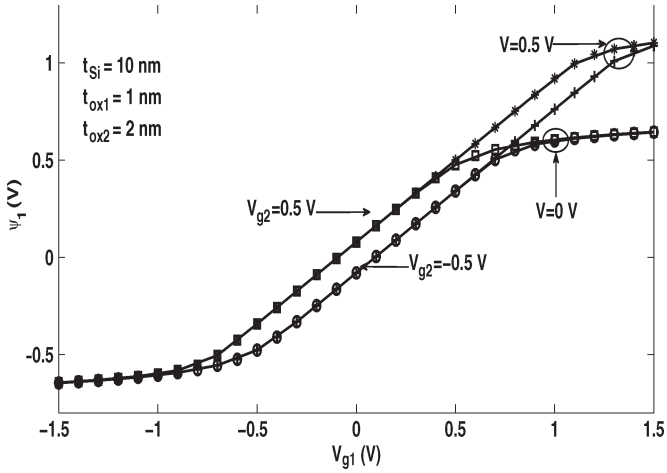

Fig. 2. Comparison of ψ_1 variation predicted by the (line) analytical against (symbols) numerical solution. V_{g1} is varied from -1.5 to 1.5 V with V_{g2} and V as parameters. Symbols used for various bias conditions are as follows: circle for ($V_{g2} = -0.5$ V; $V = 0$ V), plus for ($V_{g2} = -0.5$ V; $V = 0.5$ V), square for ($V_{g2} = 0.5$ V; $V = 0$ V), and star for ($V_{g2} = 0.5$ V; $V = 0.5$ V).

$\max(\psi_{\mathrm{lt-hyp1}}, \psi_{\mathrm{sing-hyp1}})$. Here, $\psi_{\mathrm{lt-hyp1}}$ and $\psi_{\mathrm{sing-hyp1}}$ are the roots of (16) and (17) respectively.

$$f^{\mathrm{BP}}_{\mathrm{lt-hyp1}} = \left[\frac{C_{\mathrm{ox2}}}{\varepsilon_{\mathrm{si}}}\frac{(V_{g2}-\psi_1)}{(\frac{C_{\mathrm{ox2}}}{C_{\mathrm{si}}}+1)}\right]^2 - \left[\frac{C_{\mathrm{ox1}}}{\varepsilon_{\mathrm{si}}}(V_{g1}-\psi_1)\right]^2 + 2Ae^{(\beta\frac{V}{2})}\left[\cosh\left(\beta\left(\psi_1-\frac{V}{2}\right)\right)-1\right] = 0 \tag{16}$$

$$\left[F(t_1,k_1) - \beta t_{\mathrm{si}}\sqrt{\frac{Ae^{\beta\frac{V}{2}}}{1-k_1^2}}\right] \pm F\left(\frac{\pi}{2},k_1\right) = 0. \tag{17}$$

Equation (16) results when G_1^{BP} becomes very large (k_1 approaches unity) in the *hyperbolic-BP* IVE form (11), and (17) determines the location of the singularity point $\mathrm{cn}(u_1,k_1)=0$. For the *trigonometric-BP* region ($G_1^{\mathrm{BP}} \le 0$), the root $\psi^{\mathrm{BP}}_{\mathrm{1lt-trig}}$ of $f^{\mathrm{BP}}_{\mathrm{lt-trig1}}$ in (18) gives the upper limit of the solution space with $\psi^{\mathrm{BP}}_{\mathrm{gzp1}}$ being the lower limit. Equation (18) corresponds to the location of the singularity point $\mathrm{sn}(u_1,k_1)=0$ for (13)

$$f^{\mathrm{BP}}_{\mathrm{lt-trig1}} = F(t_1,k_1) + \eta_1\frac{\beta}{2}t_{\mathrm{si}}\sqrt{\frac{Ae^{\beta\frac{V}{2}}}{k_1}} - 2F\left(\frac{\pi}{2},k_1\right) = 0. \tag{18}$$

In Figs. 1 and 2, we have validated our proposed model against the numerical solution of the PE as obtained from COMSOL Multiphysics software [11]. In Fig. 3, we show the difference between $\psi^{\mathrm{BP}}_{\mathrm{gzp1}}$ and $\psi^{\mathrm{UP}}_{\mathrm{gzp1}}$ and $V^{\mathrm{BP}}_{g2\mathrm{crit}}$ and $V^{\mathrm{UP}}_{g2\mathrm{crit}}$ and the absolute error between ψ_1^{BP} and ψ_1^{UP}. As seen from the figure, the differences between the corresponding quantities increase rapidly with decreasing gate voltage, thereby indicating the inadequacy of the unipolar approximation to the PE for gate voltages near flatband condition.

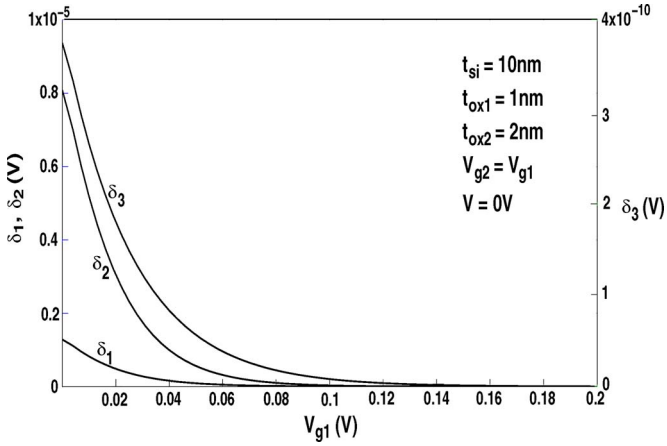

Fig. 3. Variation in $\delta_1 = |\psi^{\mathrm{BP}}_{\mathrm{gzp1}} - \psi^{\mathrm{UP}}_{\mathrm{gzp1}}|$, $\delta_2 = |V^{\mathrm{BP}}_{g2\mathrm{crit}} - V^{\mathrm{UP}}_{g2\mathrm{crit}}|$, and $\delta_3 = |\psi_1^{\mathrm{BP}} - \psi_1^{\mathrm{UP}}|$ with gate bias. The left y-axis denotes the variation in δ_1 and δ_2, while the right y-axis denotes the variation in δ_3. $V_{g2} = V_{g1}$ is swept from 0 to 0.2 V with $V = 0$ V.

III. Conclusion

A set of new IVEs for IDG MOSFET, valid from accumulation to inversion regime, has been proposed and validated against numerical solution for different bias conditions.

References

[1] S. Jandhyala, R. Kashyap, C. Anghel, and S. Mahapatra, "A simple charge model for symmetric double-gate MOSFETs adapted to gate-oxide-thickness asymmetry," *IEEE Trans. Electron Devices*, vol. 59, no. 4, pp. 1002–1007, Apr. 2012.

[2] S. Jandhyala, A. Abraham, C. Anghel, and S. Mahapatra, "Piecewise linearization technique for compact charge modeling of independent DG MOSFET," *IEEE Trans. Electron Devices*, vol. 59, no. 7, pp. 1974–1979, Jul. 2012.

[3] G. Dessai, W. Wu, B. Bakkaloglu, C. C. McAndrew, and G. Gildenblat, "Compact model and circuit simulations for asymmetric independent gate FinFETs," *J Comput. Electron.*, vol. 9, no. 3/4, pp. 103–107, Dec. 2010.

[4] G. Dessai, W. Wu, and G. Gildenblat, "Compact charge model for independent-gate asymmetric DGFET," *IEEE Trans. Electron Devices*, vol. 57, no. 9, pp. 2106–2115, Sep. 2010.

[5] A. Sahoo, P. K. Thakur, and S. Mahapatra, "A computationally efficient generalized Poisson solution for independent double gate transistors," *IEEE Trans. Electron Devices*, vol. 57, no. 3, pp. 632–636, Mar. 2010.

[6] J. Victory, Z. Yan, G. Gildenblat, C. McAndrew, and J. Zheng, "A physically based, scalable MOS varactor model and extraction methodology for RF applications," *IEEE Trans. Electron Devices*, vol. 52, no. 7, pp. 1343–1353, Jul. 2005.

[7] X. Zhou, Z. Zhu, S. C. Rustagi, G. H. See, G. Zhu, S. Lin, C. Wei, and G. H. Lim, "Rigorous surface-potential solution for undoped symmetric

double-gate MOSFETs considering both electrons and holes at quasi nonequilibrium," *IEEE Trans. Electron Devices*, vol. 55, no. 2, pp. 616–623, Feb. 2008.

[8] G. Dessai and G. Gildenblat, "Inclusion of the accumulation region in the compact models of bulk and SOI FinFETs," *IEEE Trans. Electron Devices*, vol. 58, no. 8, pp. 2644–2651, Aug. 2011.

[9] A. Milton and A. Stegun Irene, *Handbook of Mathematical Functions With Formulas, Graphs, and Mathematical Tables*. New York: Dover, p. 569.

[10] S. Jandhyala and S. Mahapatra, "An efficient robust algorithm for the surface potential calculation of independent DG MOSFET," *IEEE Trans. Electron Devices*, vol. 56, no. 6, pp. 1663–1671, Jun. 2011.

[11] COMSOL AB, User's Manual of Comsol Multiphysics, Stockholm, Sweden, 2011.

Aby Abraham received the M.Eng. degree in microelectronics system from the Indian Institute of Science, Bangalore, India, in 2012.

He is currently working as a Component Design Engineer at Intel Technology India Pvt. Ltd., Bangalore.

Pankaj Kumar Thakur received the M.Eng. degree from the Birla Institute of Technology and Science, Pilani, India, in 2008. He is currently working toward the Ph.D, degree in the Indian Institute of Science, Bangalore, India.

Santanu Mahapatra (M'08–SM'10) received the Ph.D. degree from the Ecole Polytechnique Federale de Lausanne, Lausanne, Switzerland, in 2005.

He is currently an Associate Professor with the Indian Institute of Science, Bangalore, India.